Chemistry and Physics of Lipids 222 (2019) 15–22

Contents lists available at ScienceDirect

Chemistry and Physics of Lipids

journal homepage: www.elsevier.com/locate/chemphyslip

The sphingolipidome of the model organism *Caenorhabditis elegans*

Victoria Hänel[a], Christian Pendleton[a], Michael Witting[a,b,*]

[a] Research Unit Analytical BioGeoChemistry, Helmholtz Zentrum München, Ingolstädter Landstraße 1, 85674 Neuherberg, Germany
[b] Chair of Analytical Food Chemistry, Technische Universität München, Maximus-von-Imhof-Forum 2, 85354 Freising, Germany

ARTICLE INFO

Keywords:
Caenorhabditis elegans
Lipidomics
Sphingolipids
UPLC-UHR-ToF-MS

ABSTRACT

Sphingolipids are important lipids and integral members of membranes, where they form small microdomains called lipid rafts. These rafts are enriched in cholesterol and sphingolipids, which influences biophysical properties. Interestingly, the membranes of the biomedical model organism *Caenorhabditis elegans* contain only low amounts of cholesterol. Sphingolipids in *C. elegans* are based on an unusual C17iso branched sphingoid base. In order to analyze and the sphingolipidome of *C. elegans* in more detail, we performed fractionation of lipid extracts and depletion of glycero- and glycerophospholipids together with in-depth analysis using UPLC-UHR-ToF-MS. In total we were able to detect 82 different sphingolipids from different classes, including several isomeric species.

1. Introduction

Sphingolipids are important lipids and integral members of membranes, where they are included in so called lipid rafts, small microdomains within the membrane (Simons and Ikonen, 1997; Lingwood and Simons, 2010). Lipid rafts from the biomedical model organism *Caenorhabditis elegans* have been isolated and proteins contained in these rafts have been analyzed, but so far no detailed analysis of the lipid composition has been conducted (Sedensky et al., 2004; Rao et al., 2011). In contrast to mammals, *C. elegans* membranes contain only low amounts of cholesterol, another important part of lipid rafts (Merris et al., 2003).

Sphingolipids have been linked to different important aspects in the biology of *C. elegans*. Nomura et al. have shown that ceramide glucosyltransferases are involved in the formation of oocytes and in early embryonic cell division. *C. elegans* harbors three genes encoding ceramide glucosyltransferases, names *cgt-1*, *-2*, and *-3*, of which CGT-3 shows the highest enzymatic activity. RNAi of *cgt-1/cgt-3* is lethal at the L1 stage (Nomura et al., 2011). The results showed that glucosylceramides (GlcCers) are required for postembryonic development. Monomethyl branched chain fatty acids (mmBCFAs) have been also linked to *C. elegans* development (Kniazeva et al., 2004). Sphingolipids in *C. elegans* are based on a unusual C17iso branched chain sphingoid base (Chitwood et al., 1995). This sphingoid base is derived from the reaction of the mmBCFA 13-methyl myristic acid (C15iso) with Serine. Hannich et al. have shown by isotope labeling that the sphingoid bases are derived from Leucine (Hannich et al., 2017). Indeed, > 99% of mmBCFAs are produced by C. elegans itself (Perez and Van Gilst, 2008). The N-acyl bound fatty acid are usually 2-hydroxy modified and have a length between C20 and C26 in glucosylceramides (Chitwood et al., 1995; Gerdt et al., 1997). Zhu et al. have shown that GlcCers form together with TORC1, a signaling pathway, to coordinate nutrient status and metabolism during growth and development (Zhu et al., 2013).

Sphingolipids have been also linked to autophagy-dependent lifespan extension. Mosbech et al. found that loss of *hyl-1* and *lagr-1* extend the lifespan in an *atg-12* dependent manner. Additionally, *pha-4*, *daf-16* and *skn-1* are also required. *hyl-1*, *-2* and *lagr-1* are ceramide synthases catalyzing the transfer of an acyl group from acyl-CoA to a N-acyl. In this reaction *hyl-1* seems to have preference for acyl chains with 24 or more carbons, while *hyl-2* prefers 22 carbons and shorter (Mosbech et al., 2013). Additionally, *hyl-2* was shown to be protective in anoxia, because loss of *hyl-2* increases sensitivity of *C. elegans* to anoxia. In contrast to this *hyl-1* loss of function lead to more resistance (Menuz et al., 2009).

These examples demonstrate different species of a certain class play important and often opposing roles and that sphingolipid classes cannot be treated as homogenous entities. A putative biosynthetic pathway of different sphingolipids is shown in Fig. 1A, adapted from (Watts and

Abbreviations: DhCers, dihydroceramides; Cers, ceramides; DhSMs, dihydrosphingomyelins; SMs, sphingomyelins; GlcCers, glucosylceramides; HexCers, hexosylceramides; UPLC-UHR-ToF-MS, ultrahigh performance liquid chromatography – ultrahigh resolution – time of flight – mass spectrometry; MeOH, methanol; ACN, acetonitrile; iPrOH, 2-propanol; $CHCl_3$, chloroform; mmBCFA, monomethyl branched chain fatty acid

* Corresponding author at: Research Unit Analytical BioGeoChemistry, Helmholtz Zentrum München, Ingolstädter Landstraße 1, 85674 Neuherberg, Germany.
E-mail address: michael.witting@helmholtz-muenchen.de (M. Witting).

https://doi.org/10.1016/j.chemphyslip.2019.04.009
Received 11 February 2019; Received in revised form 18 April 2019; Accepted 23 April 2019
Available online 24 April 2019
0009-3084/

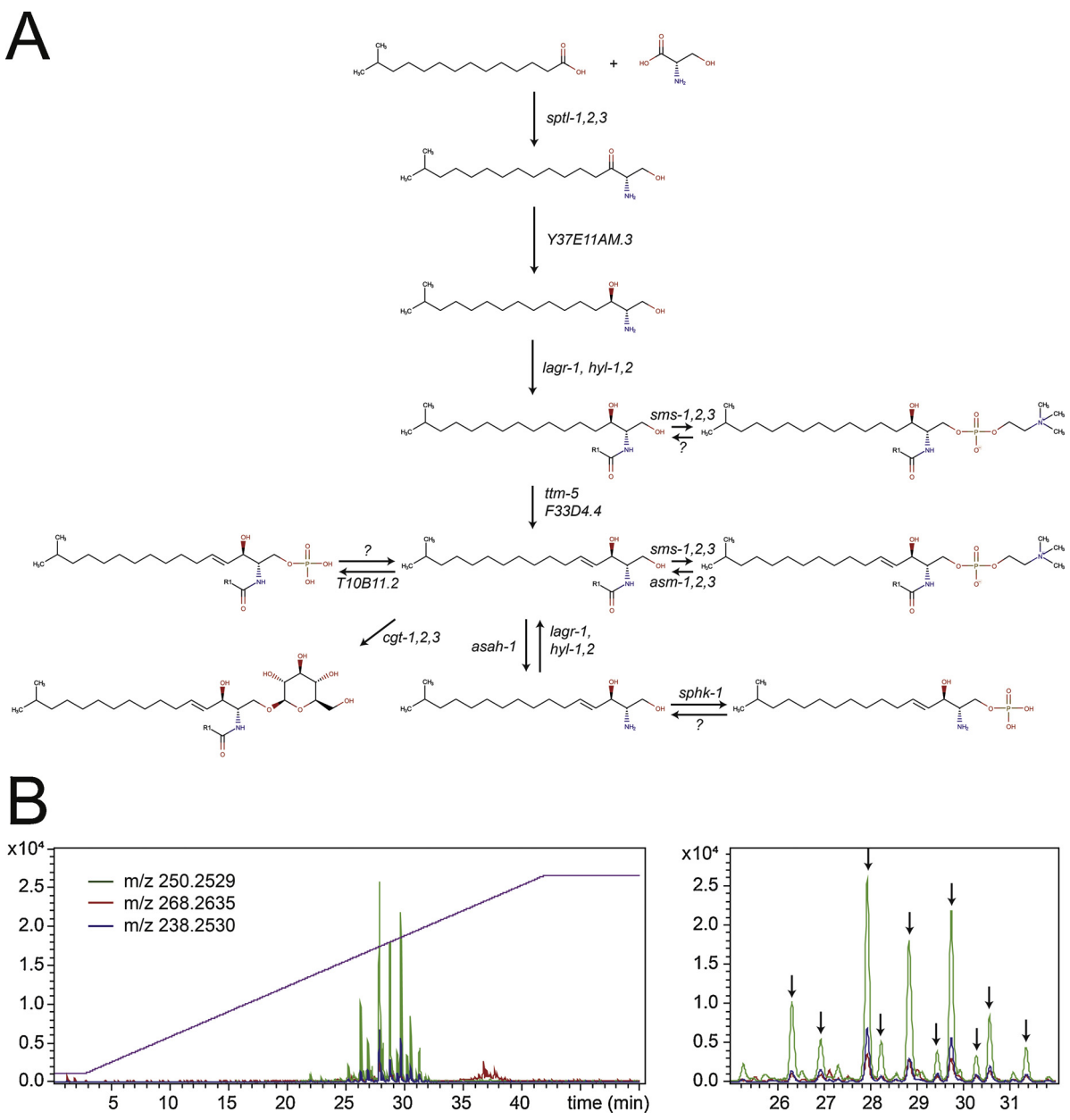

Fig. 1. (A) Biosynthetic pathway of sphingolipids in C. elegans, adapted from (Watts and Ristow, 2017). Known genes that participate in the synthesis of different sphingolipids are indicated. For simplification cofactors and other participating metabolites, e.g. fatty acyls CoAs are not shown. (B) hrEICs of common fragment masses indicating the presence of C17 sphingoid bases using bbCID fragmentation. Arrows indicate examples of the co-elution of three fragment masses attributed to the C17 sphingoid base.

Ristow (2017)). So far, no definite number of sphingolipids in *C. elegans* is known. Given the need for more detailed (routine) analysis of sphingolipids in *C. elegans* it is important to define the sphingolipidome of this organism.

Here we describe structural analysis of sphingolipids from wildtype *C. elegans*. We performed UPLC-UHR-ToF-MS analysis to detect members of the sphingolipid class and perform partial structural elucidation of intact sphingolipids. By combining data independent and date dependent fragmentation together with *in silico* prediction of potential sphingolipid structures we could putatively identify 82 sphingolipids, including several isomeric species, in wild type *C. elegans* extracts. Identification was performed to the hydroxyl group and/or fatty acyl level according to the shorthand notation by (Liebisch et al. (2013)). Putative identifications can be used in future sphingolipidomics approaches in the worm and will advance our knowledge on the regulation of sphingolipid metabolism and potentially lipid rafts formation and function in *C. elegans*.

2. Material and methods

2.1. Chemicals

Methanol (MeOH), 2-Propanol (iPrOH), Acetonitril (ACN) were of LC–MS grade (Sigma-Aldrich, Taufkirchen, Germany). All other solvents and chemicals were of the highest available purity, usually analytical grade. Water was purified on Merck Millipore Integral 3 water purification system with TOC < 3 ppb, 18 MOhm.

2.2. C. elegans cultivation

C. elegans were grown in liquid culture to obtain sufficient biomass. Worms were grown in S-medium at 20 °C and fed with concentrated

Escherichia coli NA22. Worms were regularly checked and *E. coli* NA22 was added to prevent starvation. After one week, worms were harvested and separated from bacteria by filtration using a 2.7 µm Millipore glass-fiber filter (Sigma-Aldrich, Taufkirchen, Germany). After two times of washing with 10 mL cold M9, worms were frozen at -80 °C until extraction and analysis.

2.3. Lipid extraction

Lipids were extracted according to the Folch method (Folch et al., 1957). A pellet of about 750 mg (wet weight) of mixed stage worm samples was mixed with 1 mL of MeOH and homogenized in a Precellys Evolution bead beater (Bertin Instruments, Montigny-le-Bretonneux, France) at about 0 °C and 8000 rpm for three times 10 s with 20 s pause between. After addition of 2 mL $CHCl_3$ the sample was shaken for one hour at room temperature and 500 rpm using an Eppendorf ThermoMixer C (Eppendorf, Hamburg, Germany). Phase separation was induced by addition of 1 mL H_2O and centrifugation at an RCF of 15294 × g and 4 °C for 15 min. The polar phase was re-extracted with 2 mL of $CHCl_3$ / MeOH / H_2O (v/v, 86 / 14 / 1) for 15 min. After phase separation organic phases were combined and dried in two aliquots in a SpeedVac Savant centrifugal evaporator (Thermo Scientific, Dreieich, Germany). One aliquot was re-dissolved in 50 µL iPrOH / ACN / H_2O (v/v, 60 / 35 / 5) prior to analysis with UPLC-UHR-ToF-MS and the other in $CHCl_3$ for lipid fractionation.

2.4. Sphingolipid fractionation

Sphingolipids were fractionated according to Bodennec (Bodennec et al., 2000). Briefly, different sphingolipids were eluted from either separated or piggy-backed LC-NH_2 (Supelclean LC-NH_2 SPE tubes, 1 mL, 100 mg sorbent, Supelco) and LC-WCX (Supelclean LC-WCX SPE tubes, 1 mL, 100 mg sorbent) SPE columns. 8 different solvent mixtures were used to obtain 7 fractions. Fractionation was exactly performed as described in (Bodennec et al., 2000).

2.5. Glycero- and glycerophospholipid depletion

Depletion of glycerol- and glycerophospholipids was adapted from (Shaner et al., 2009).A 50 µL aliquot of lipidome fractions was dried and resuspended in 450 µL MeOH and 50 µL 1 M KOH in MeOH. The samples were incubated at 37 °C for 2 h in a Thermomixer and shaken at 1000 rpm. After this time samples were neutralized with glacial acetic acid (˜ 1 µL) and 1000 µL $CHCl_3$ were added and the sample shaken at 1000 rpm and 20 °C for 1 h. After addition of 500 µL H_2O, samples were vortexed and phases separated by centrifugation. The lower organic phase was dried in a SpeedVac and redisolved in 50 µL iPrOH / ACN / H_2O (v/v, 60 / 35 / 5) for UPLC-UHR-ToF-MS analysis.

2.6. UPLC-UHR-ToF-MS analysis

Analysis of lipids was performed according to (Witting et al. (2014)). Briefly, a Waters Acquity UPLC (Waters, Eschborn, Germany) was coupled to a Bruker maXis UHR-ToF-MS (Bruker Daltonic, Bremen, Germany). Separation of lipids was achieved on a Waters Cortecs C18 column (150 mm × 2.1 mm ID, 1.7 µm particle size) (Waters, Eschborn, Germany) using a gradient from eluent A (60% ACN / 40% H_2O + 10 mM NH_4HCO_2 + 0.1% formic acid (v/v)) to eluent B (90% iPrOH / 10% ACN + 10 mM NH_4HCO_2 + 0.1% formic acid (v/v)). Analysis was performed in positive and negative ionization mode. In contrast to the described method, the gradient time was doubled for high resolving power to detected individual lipids and increase separation of isomeric species. Gradient conditions were as followed: After an isocratic step of 32% B for 3 min a linear increase to 97% B in 39 min was performed with an isocratic hold of 97% B for 7 min. After return to initial conditions the column was re-equilibrated for 5 min with the starting conditions.

Mass spectrometric settings were as followed: Nebulizer 2.0 bar, Dry Gas 10.0 L/min, Dry Temp 200 °C, Capillary Voltage 4000 V and End Plate Offset 500 V. Mass range was set from *m/z* 100 to *m/z* 2000. 1:4 diluted Low Concentration Tuning Mix (Agilent Technologies, Waldbronn Germany) was injected via a 6-port valve prior to each analysis for individual recalibration of *m/z* axis.

Fragmentation data was either collected in data-independent (broad band Collision Induced Dissociation, bbCID) or data-dependent (AutoMSn) acquisition mode. 40 eV were used as collision energy for bbCID, while for AutoMSn composite spectra of 10 and 40 eV were collected.

2.7. In silico sphingolipid structure generation

Sphingolipid structures have been generated using the JChem for Excel Plugin (ChemAxon, Budapest, Hungary). Template reactions have been manually drawn and the JCReactProductStructure() reaction function in JChem for Excel was used to generate product structures. SMILES representation of fatty acid and sphingoid bases were used as input (SI Tables 1 and 2). SMILES, InChIs and InChIKeys were generated using the JCMolFormat() function in JChem for Excel. Where available, ChEBI, LipidMaps and SwissLipids IDs have been added. The full table of structures is available in the SI (SI Tables 3–8).

3. Results and discussion

3.1. Screening for sphingoid backbones

Sphingolipids in *C. elegans* contain an unusual d17:1 iso sphingoid base (Chitwood et al., 1995). This sphingoid base is prodduced from 15:0iso fatty acid (FA(14:0(13Me), 13-methyl myristic acid) and serine. Additionally, Hannich et al have shown that the enzyme serine palmitoyl transferase (SPT) in *C. elegans* can also accept alanine, which produces a 1-deoxy sphingoid base (Hannich et al., 2017). In order to get an impression on the sphingoid bases in complex lipids we performed data independent fragmentation (broad band Collision Induced Dissociation, bbCID) in positive ionization mode. Typical fragmentation of sphingolipids yields a long chain base fragment $[LCB\text{-}H_2O]^+$ and the respective fragment plus an additional loss of H_2O (−18 Da) and loss of water and CH_2O (−48 Da). We generated extracted ion chromatograms (EICs) with an error of 0.005 Da for the MS^2 trace on the respective masses for d17:0iso, d17:1iso, -m17:0iso, m17:1iso sphingoid bases. A signal to noise (S/N) threshold of 25 and higher was required for the fragment *m/z* coeluting with the lowest intensity. As negative control we also searched for d18:0 and d18:1 sphingoid bases, which are not produced *C. elegans* (Chitwood et al., 1995; Hannich et al., 2017). We only observed peaks for d17:1 sphingoid base, derived from the loss of *N*-acyls as ketene. In our data the highest observed peak is the sphingoid base fragment – 2 x H_2O (*m/z* 250.2529), followed by the fragment – H_2O and CH_2O (*m/z* 238.2529) and the sphingoid base fragment – H_2O (*m/z* 268.2635) (Fig. 1B). Since MS cannot separate between straight and branched chains with employed methodology, we identified the sphingoid bases C17. Our results confirm previous findings that *C. elegans* only uses C17 sphingoid bases.

3.2. In silico generation of sphingolipid structures

Next, we investigated potential structures for *C. elegans* sphingolipids. We detected *m/z* values identifying C17 sphingoid base in *C. elegans*. Previously performed detailed analysis of sphingoid bases in *C. elegans* identified C17iso branched chain sphingoid bases (Hannich et al., 2017). We therefore assume for the rest of the manuscript either d17:0iso or d17:1 iso as sphingoid base. At the current stage, LipidMaps does only contain a few sphingolipids containing a C17 sphingoid base and does not contain sphingolipids with a C17iso branched chain

sphingoid base (Sud et al., 2007). We generated *in silico* all possible structures based on d17:0iso and d17:1iso sphingoid backbones. *C. elegans* is able to synthesize a large range of fatty acids on its own, including branched chain, mono- and polyunsaturated fatty acids. Different publications have investigated the fatty acid composition of *C. elegans* (Watts and Browse, 2002; Owopetu et al., 2016). However, most of these works focused on the total lipid composition and not specifically on sphingolipids. Chitwood et al. and Gerdt et al. specifically analyzed the composition of glycosphingolipids and found that many of them contain even and odd long chain 2-hydroxy fatty acids (Chitwood et al., 1995; Gerdt et al., 1997). Zhu et al. also reported the dependence of a sphingolipid dependent phenotype on *fath-1*, which produces 2-hydroxy fatty acids (Zhu et al., 2013; Li et al., 2018).

We therefore generated sphingolipids from two different sets of input fatty acids. The first one, called “standard fatty acids”, is based on commonly observed fatty acids described in literature to be present in *C. elegans* (Watts and Browse, 2002; Vrablik et al., 2015; Henry et al., 2016) and usually make up glycero- and glycerophospholipids, and the second one is called “2-hydroxy and related fatty acids”. The second group contained non-hydroxylated and 2-hydroxy fatty acids of length as described by Chitwood et al. and (Chitwood et al., 1995; Gerdt et al. (1997)). Table 1 summarizes the used fatty acids with their shorthand notation. A full list with all molecular formulae and, InChIKeys and ChEBI identifiers are found in SI Tables 1 and 2.

We generated structures for dihydroceramides (DhCers), ceramides (Cers), dihydrosphingomyelins (DhSMs), sphingomyelins (SMs), ceramide-1-phosphates (C1Ps) and glucosylceramides (GlcCers). In total we obtained 510 sphingolipids at a full structural level, 324 at the fatty acyl level and 282 at the hydroxyl group level, according to the nomenclature by (Liebisch et al. (2013)). Initial screening of the data obtained data showed that we were not able to detect DiHexCer or TriHexCers and were therefore ignored in structure generation and further analysis. Structures of all *in silico* generated sphingolipids are found in SI Table 3–8.

3.3. MS^1 screening for sphingolipid masses

Using the generated list of potential sphingolipids, we next checked for the presences of fitting *m/z* values on the MS^1 level. We filtered all sphingolipids based on the sum composition (e.g. Cer(d41:1) and unique masses and created hrEICs for the $[M+H]^+$ and $[M\text{-}H_2O+H]^+$ adducts. Since the loss of H_2O is a prominent feature we used the coelution of the $[M+H]^+$ and $[M\text{-}H_2O+H]^+$ masses criterium towards positive identification as sphingolipid. We used the odd masses of $[M+H]^+$ adducts for DhSM and SM species and also verified that these odd masses were not part of an isotope pattern of glycerophospholipids. Instead of bbCID we used data dependent acquisition of tandem MS to potentially further verify the identity of detected *m/z*. The number of putative sphingolipids identified by exact mass are summarized in Table 2. Interestingly, we detected a high number of DhSMs and SMs with fatty acids from the standard fatty acids. However, they were of very low in intensity close to the chosen S/N of 25. We were not able to detect C1Ps as well as DiHexCer and TriHexCer in whole lipid extracts.

Table 2
Number of detected peaks in whole lipid extracts with fitting masses for different predicted sphingolipids based on MS1 level.

Class	Fatty acyl group	Theoretical	Found
DhCer	Std Fatty acids	22	0
	2-OH fatty acids	32	4
Cer	Std Fatty acids	22	1
	2-OH fatty acids	32	13
DhSM	Std Fatty acids	22	7
	2-OH fatty acids	32	6
SM	Std Fatty acids	22	8
	2-OH fatty acids	32	16
HexCer	Std Fatty acids	22	0
	2-OH fatty acids	32	3

3.4. Fragmentation pattern of different sphingolipid classes

Fragmentation of sphingolipids have been extensively studied, mostly in negative ionization mode or from alkali adducts (Hsu and Turk, 2002; Hsu, 2016; Tsugawa et al., 2017; Anon., 2019; Hsu and Turk, 2000). To further identify sphingolipids of *C. elegans* we compared fragmentation pattern of sphingolipid candidates detected so far with known fragmentation patterns of different sphingolipids to derive fragmentation pathways and fragments that can be used for identification. Due to higher sensitivity we focused on the fragmentation in positive ionization mode.

Typical fragments for Cers are the loss of a water molecule, which is possible for both hydroxyl groups. This fragmentation requires low energy, since it is often already observed as in-source fragment. Both obtained structures can lose the N-Acyl, again yielding fragments of identical masses. One of these fragments is losing an additional water molecule, while the other is losing a formaldehyde. The fragments are yielding a typical peak triplet with the mass's *m/z* 238.2529, 250.2529 and 268.2635. These three fragments can identify a molecule as a sphingolipid containing a C17:1 sphingoid base. The N-Acyl can be identified by the neutral loss between the $[M+H]^+$ and $[LCB\text{-}H_2O+H]^+$ fragment or (e.g. 524.5033 – 268.2635 = 256.2398 = FA(16:0)) $[M\text{-}H_2O+H]^+$ fragment and $[LCB\text{-}2\ H_2O+H]^+$ fragment (e.g. 506.4923 – 250.2530 = 256.2393 = FA(16:0)). Fig. 2A shows a typical MS^2 spectrum from a peak identified as Cer(d17:1/16:0) and the structure of the proposed fragments (Fig. 2B).

In contrast to Cers, DhCers show the typical water loss to a lesser extent. This suggests that the loss of the hydroxyl group at position 3 is the favored one in ceramides, because of the resonance stabilizing effect (mesomerism) arising from the conjugated double bond (Anon., 2015). Additionally, *m/z* 288.2897 is observed for DhCers, which represents the loss of the fatty acyl as ketene directly from the $[M+H]^+$. Because of the missing double bond and its resonance stabilizing effect, DhCers

Table 1
Table of shorthand notations of fatty acids used for in silico generation of sphingolipid structures.

Group	Fatty acids
Standard fatty acids	FA(12:0), FA(12:0(11Me)), FA(13:0), FA(13:0(12Me)), FA(14:0), FA(14:0(12Me)), FA(14:0(13Me)), FA(15:0), FA(15:1(9Z,14Me)), FA(16:1(11Z)), FA(16:1(9Z)), FA(15:0(14Me)), FA(16:0), FA(17:1(10Z)), FA(16:0(14Me)), FA(16:0(15Me)), FA(17:0), FA(18:4(6Z,9Z,12Z,15Z)), FA(18:3(6Z,9Z,12Z)), FA(18:3(9Z,12Z,15Z)), FA(18:2(9Z,12Z)), FA(18:1(11Z)), FA(18:1(9Z)), FA(17:0(16Me)), FA(18:0), FA(19:1(10Z)), FA(19:0), FA(20:5(5Z,8Z,11Z,14Z,17Z)), FA(20:4(5Z,8Z,11Z,14Z)), FA(20:4(8Z,11Z,14Z,17Z)), FA(20:3(8Z,11Z,14Z)), FA(20:2(11Z,14Z)), FA(20:1(11Z)), FA(20:1(13Z)), FA(20:1(9Z)), FA(20:0), FA(22:0)
2-hydroxy and related fatty acids	FA(16:0), FA(18:0), FA(20:0), FA(22:0), FA(24:0), FA(26:0), FA(28:0),FA(30:0), FA(16:0(2OH)), FA(18:0(2OH)), FA(20:0(2OH)), FA(22:0(2OH)), FA(24:0(2OH)), FA(26:0(2OH)), FA(28:0(2OH)), FA(30:0(2OH)), FA(14:0(13Me)), FA(16:0(15Me)), FA(18:0(17Me)), FA(20:0(19Me)), FA(22:0(21Me)), FA(24:0(23Me)), FA(26:0(25Me)), FA(28:0(27Me)), FA(14:0(13Me,2OH)), FA(16:0(15Me,2OH)), FA(18:0(17Me,2OH)), FA(20:0(19Me,2OH)), FA(22:0(21Me,2OH)), FA(24:0(23Me,2OH)), FA(26:0(25Me,2OH)), FA(28:0(27Me,2OH)), FA(15:0), FA(17:0), FA(19:0), FA(21:0), FA(23:0), FA(25:0), FA(27:0), FA(29:0), FA(15:0(2OH)), FA(17:0(2OH)), FA(19:0(2OH)), FA(21:0(2OH)), FA(23:0(2OH)), FA(25:0(2OH)), FA(27:0(2OH)), FA(29:0(2OH))

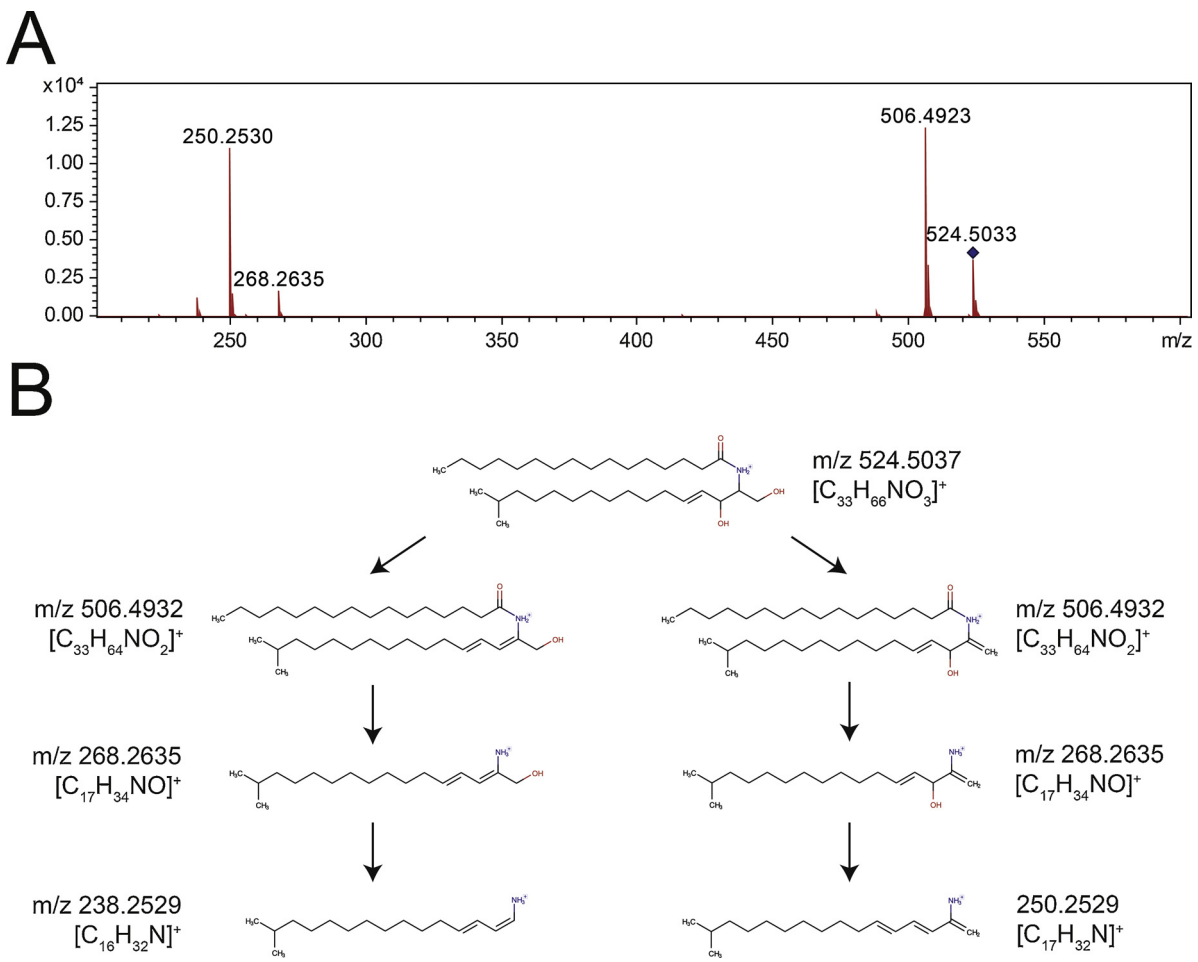

Fig. 2. (A) Example MS/MS spectrum of Cer(d17:1/16:0). Major peaks are the [M − H2O + H] + fragment as well as *m/z* 250.2530. (B) Proposed fragmentation pathway for C. elegans ceramides. Two possibilities for loss of water from the parent ion are possible, yielding two different fragmentation trees.

tend to show lower intensities for the $[M\text{-}H_2O+H]^+$ fragment. Interestingly, DhCers show a N-Acyl fragment, which correspond to a N-Acyl amide. These fragments can be also found in of highly abundant Cer fragmentation spectra, but only at low intensities.

Similar N-Acyl amide fragments as the ones observed for DhCers were found in GlcCers. GlcCers showed different fragments related to the loss of the hexosyl headgroup. Neutral losses of 162 were observed from the $[M+H]^+$ and $[M\text{-}H_2O+H]^+$ peak.

DhSMs and SMs yield a fragment of *m/z* 184.07 corresponding the phosphocholine headgroup. This was the only observed fragment and therefore no further structural characterization was possible for SMs.

3.5. Fractionation of lipidomes using SPE

In order to analyze the sphingolipids in more detail and to perform detailed tandem MS for identification without interference from overlapping glycerol- or glycerophospholipids we fractionated our lipid extract according to (Bodennec et al. (2000)). This methodology uses two SPE column, NH_2 and WCX, to fractionate lipids into 7 fractions. For this study fractions 2, 4, 5, 6 and 7 were of particular interest containing free DhCers and Cers, neutral glycosphingolipids (HexCer, DiHexCer and TriHexCer), sphingosines, DhSMs and SMs and C1Ps respectively. To further remove overlapping interferences from remaining glycerophospholipids they were saponified and the dried fractions were reconstituted with methanolic KOH. We used the mass list derived from the 2-OH fatty acids. Additionally, we included these masses in the preference list for data dependent fragmentation to obtain MS^2 fragmentation data to confirm the identity of sphingolipids.

With the fractionation and saponification, we were able to detect more sphingolipid species compared to the whole Folch extract, especially low abundant species suppressed by other co-eluting lipids. However, we were not able to detect any C1Ps, DiHexCers or TriHexCers species in the respective fractions. All of them might be too low in concentration and were excluded from further discussion. While Gerdt et al. detected di- and trihexosyl ceramides they used 10 g of dried biological material and obtained about 550 mg of lipid extract. Furthermore, they used a different methodology and analytical methods. Since C1Ps, DiHexCer and TriHexCers represent polar lipids, which show no good retention behavior and peak shapes on reversed phase column. We also could not identify any species of these sphingolipid classes in the polar phases of the lipid extraction (data not shown). We conclude that either a larger number of worms or more sensitive or different methods are required for the detection of these sphingolipid classes.

For different DhCers, Cers and HexCers already with the MS^1 screen we detected several chromatographic double peaks for the same mass which are mostly different by about 0.3 min in their retention time. We are assuming that the different peaks are derived from either straight or branched chain fatty acid isomers with the same number of carbons. Calculating the logP value for the respective species, branched chain derivates have always the smaller logP, although the difference is not large. The earlier eluting peak would represent the branched chain version and it usually represents the small peak when peak areas are compared. Using MS^2 we could not find any differences in the fragmentation behavior of the two different peaks. One further explanation of these minor peaks would be the presence of sphingolipids with a

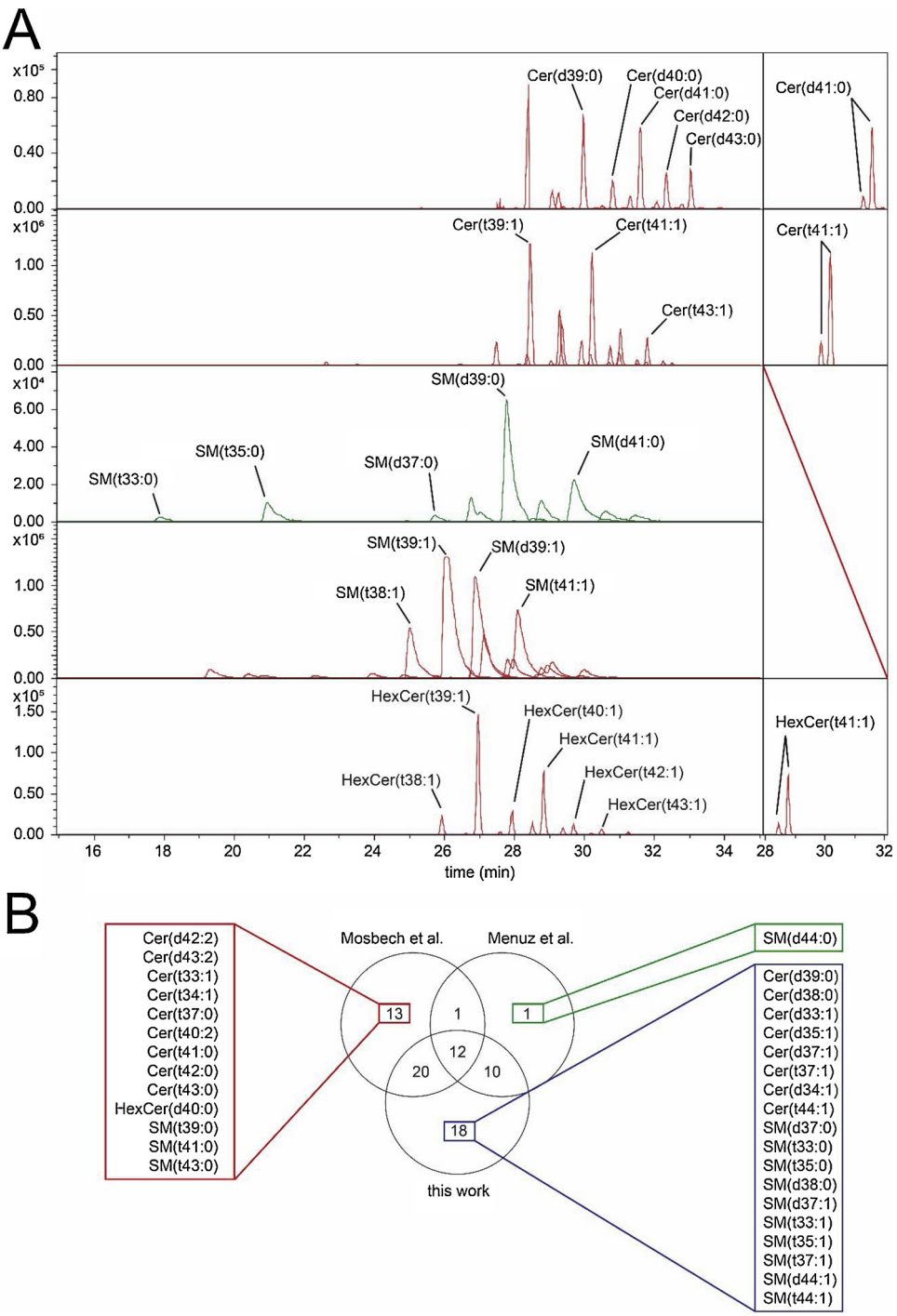

Fig. 3. (A) Extracted ion chromatograms of detected sphingolipids. Peaks are annotated with their putative annotation on the MS1 level. MS/MS identified that all the detected peaks shown in this figure contain a C17 sphingoid base. (B) Venn diagram showing the overlap between sphingolipid species detected by Mosbech et al., Menuz et al. and this paper. Unique sphingolipids for each publication are indicated.

t17:0 sphingoid base. These sphingoid bases tend to loss water molecules in the source due to high potentials used in ESI. This would make the molecule indistinguishable from d17:1 based sphingolipids except for slightly different retention times. We checked for the presence of *m/z* values (even at low intensities) indicative for t17:1 but could not find any evidence for the presence of this sphingoid base. Chitwood et al. and detected different iso branched chain fatty acids in glucosylceramides, including even chained iso fatty acids along with straight chain fatty acids. Particularly, an iso C24:0(OH) fatty acid accounted for 3.3% relative amount, while the straight chain isomer C24:0(OH) for 17.5% in the publication of Gerdt et al. (1997). Similar trends were found for HexCers containing C23:0(OH) and C25:0(OH). Due to missing standards no verification if the peaks represent either t17:0 or isomeric N-Acyl species was possible.

In the next step we compared the different fatty acids bound as N-Acyl across the different detected sphingolipid classes. Compared to the other detected sphinoglipids, HexCers show a very specific fatty acid profile. We found that hexosylceramides contain exclusively hydroxy fatty acids. While Gerdt et al. detected also C16, C18:1 and C18:0 fatty acids in the glucosylceramides, we were not able to find them. Consistent with previous findings the most prominent lipid contains a C22:0(OH) fatty acyl (Gerdt et al., 1997; Mosbech et al., 2013).

Likewise, Mosbech et al. also detected only HexCers containing three hydroxyl groups (Mosbech et al., 2013). Only C21-C6 fatty acids were detected. It was shown that HexCers in *C. elegans* contain a β-D-Glucose (Gerdt et al., 1997). Mosbech et al. have shown that *hyl-1* is required for synthesis of very long chain fatty acids (> = C24) and *hyl-2* produces ceramides with shorter chain acyl (< = C22). A similar substrate specificity might exist for glucosyltransferases, accepting only 2-hydroxy fatty acyl containing sphingolipids of a specific length with the highest activity towards C22. The worm harbors three ceramide glucosyltransferases, *cgt-1* to *-3*, whereas *cgt-3* was shown to have the highest activity (Nomura et al., 2011). No substrate specificity regarding bound n-acyls have been shown so far for these three enzymes but looking at the fatty acid distribution it might be possible that they only use specific Cers, the fatty acid distribution of sphingomyelins mirrors the distribution of Cers with a few exceptions. A list with all detected sphingolipids is available in SI Tables 9 and 10.

It will be of great importance in future to determine the substrate specificity of different enzymes involved in biosynthesis and degradation of sphingolipids. Several publications treat the individual classes as single entities. However, each class contains several individual species, each with slightly different physicochemical properties. These properties influence the activity of individual lipids and their function in defined lipid rafts. Furthermore, it is interesting why *C. elegans* uses d17:1iso sphingoid bases and why their membranes contain only low levels of cholesterol (Merris et al., 2003).

3.6. Comparison against previous detected sphingolipids

In total we were able to detect 82 different sphingolipids, including several isomeric species, in our sample based on extensive fractionation, saponification and analysis with UPLC-UHR-ToF-MS. Sphingolipids have been previously analyzed in different conditions in *C. elegans*. Mosbech et al. found that different ceramide synthetases have opposing roles on the lifespan of *C. elegans*. They detected in total 46 sphingolipids from Cers, SMs and HexCers (Mosbech et al., 2013). Menuz et al. have shown that *hyl-2* is protective against anoxia in *C. elegans*. They quantified 12 Cers and 12 SMs (Menuz et al., 2009). Since only nominal masses are presented, we selected the closest matching sphingolipid from our list. Furthermore, Cutler et al. performed analysis of sphingolipids in *C. elegans*. However, from their presented results it is not possible to deduce which lipid species were used as a basis (d17iso or d18 sphingoid bases). We therefore neglected their results for a comparative analysis (Cutler et al., 2014).

We compared the sphingolipids previously detected with our obtained list. For this comparison the sum composition, e.g. Cer(t44:1) was used. This reduced the number of sphingolipids to 60 for this publication. From all the publications 12 sphingolipids were detected in all (Fig. 3C), mostly Cers and SMs. Shared species between Mosbech and this publication are different HexCers and SMs, while with Menuz mostly Cers and SMs are common. Consistent with our own and previous finding, HexCers were found to contain in total 3 hydroxyl groups, where two are located on the sphingoid base and in the N-Acyl. HexCers containing a C22:0(OH) N-Acyl group were the highest found in this group.

In comparison to previous published papers we performed UPLC-UHR-ToF-MS, which allowed to separate potential isomers and increases ionization efficiency by separating lipid species. Additionally, performed fractionation and saponification of base sensitive lipids further enhanced efficiency. This allowed us to describe the *C. elegans* sphingolipidome in more detail. However, it remains elusive what the exact structure of the minor isomers is and if they play specific roles in lipid raft formation. So far this publication in the most comprehensive description of sphinoglipids in *C. elegans*.

4. Conclusion

Sphingolipids play important roles in the biology of *C. elegans*. In this work we describe a detailed analysis of intact sphingolipids from different classes. In total we were able to detect and confirm 82 sphingolipids, including different isomeric species. Although several genes are known, we are still missing parts of the biosynthetic pathways, e.g. which enzymes produce the very long chain fatty acids. *C. elegans* was shown to also contain ascarosides, glycolipids important in signaling, with chain length up to 30 carbons (von Reuss et al., 2017). Likewise, Gao et al. were able to detect a C30 fatty acid (Gao et al., 2017; Gao et al., 2018). So far, no biosynthetic pathway for this fatty acid has been established in *C. elegans* and no sphingolipid with such a N-acyl side chain has been detected.

Since *C. elegans* contains, compared to other mammals and normalized to PC, 20 times less cholesterol in the membrane, it will be interesting in the future to analyze sphingolipids from isolated lipid rafts. We believe that UPLC-UHR-ToF-MS will be a valuable tool for the in-depth analysis of the *C. elegans* sphingolipidome in future, since it allows a more detailed snapshot.

Appendix A. Supplementary data

Supplementary material related to this article can be found, in the online version, at doi:https://doi.org/10.1016/j.chemphyslip.2019.04.009.

References

Anon, 2015. Chapter 6 sphingolipids (SP). Tandem Mass Spectrometry of Lipids: Molecular Analysis of Complex Lipids. The Royal Society of Chemistry, pp. 194–232.

Anon, 2019. Fragmentation Patterns of Sphingolipids, in Lipidomics.

Bodennec, J., et al., 2000. 9] - purification of sphingolipid classes by solid-phase extraction with aminopropyl and weak cation exchanger cartridges. In: Merrill, A.H., Hannun, Y.A. (Eds.), Methods in Enzymology. Academic Press, pp. 101–114.

Chitwood, D., et al., 1995. The glycosylceramides of the nematodeCaenorhabditis elegans contain an unusual, branched-chain sphingoid base. Lipids 30 (6), 567–573.

Cutler, R.G., et al., 2014. Sphingolipid metabolism regulates development and lifespan in Caenorhabditis elegans. Mech. Ageing Dev. 143-144, 9–18.

Folch, J., Lees, M., Stanley, G.H.S., 1957. A simple method for the isolation and purification of total lipids from animal tissues. J. Biol. Chem. 226 (1), 497–509.

Gao, A.W., et al., 2017. A sensitive mass spectrometry platform identifies metabolic changes of life history traits in C. elegans. Sci. Rep. 7 (1), 2408.

Gao, A.W., et al., 2018. Natural genetic variation in C. elegans identified genomic loci controlling metabolite levels. Genome Res. 28 (9), 1296–1308.

Gerdt, S., et al., 1997. Isolation and structural analysis of three neutral glycosphingolipids from a mixed population of Caenorhabditis elegans (Nematoda: rhabditida). Glycobiology 7 (2), 265–275.

Hannich, J.T., et al., 2017. Structure and conserved function of iso-branched sphingoid bases from the nematode Caenorhabditis elegans. Chem. Sci. 8 (5), 3676–3686.

Henry, P., et al., 2016. Fatty acids composition of Caenorhabditis elegans using accurate mass GCMS-QTOF. J. Environ. Sci. Health B 51 (8), 546–552.

Hsu, F.-F., 2016. Complete structural characterization of ceramides as [M − H] − ions by multiple-stage linear ion trap mass spectrometry. Biochimie 130, 63–75.

Hsu, F.-F., Turk, J., 2000. Structural determination of sphingomyelin by tandem mass spectrometry with electrospray ionization. J. Am. Soc. Mass Spectrom. 11 (5), 437–449.

Hsu, F.-Fu., Turk, J., 2002. Characterization of ceramides by low energy collisional-activated dissociation tandem mass spectrometry with negative-ion electrospray ionization. J. Am. Soc. Mass Spectrom. 13 (5), 558–570.

Kniazeva, M., et al., 2004. Monomethyl branched-chain fatty acids play an essential role in Caenorhabditis elegans development. PLoS Biol. 2 (9), e257.

Li, Y., et al., 2018. *C. elegans* fatty acid two-hydroxylase regulates intestinal homeostasis by affecting heptadecenoic acid production. Cell. Physiol. Biochem. 49 (3), 947–960.

Liebisch, G., et al., 2013. Shorthand notation for lipid structures derived from mass spectrometry. J. Lipid Res. 54 (6), 1523–1530.

Lingwood, D., Simons, K., 2010. Lipid rafts as a membrane-organizing principle. Science 327 (5961), 46–50.

Menuz, V., et al., 2009. Protection of C. Elegans from anoxia by HYL-2 ceramide synthase. Science 324 (5925), 381–384.

Merris, M., et al., 2003. Sterol effects and sites of sterol accumulation in Caenorhabditis elegans: developmental requirement for 4α-methyl sterols. J. Lipid Res. 44 (1), 172–181.

Mosbech, M.-B., et al., 2013. Functional loss of two ceramide synthases elicits autophagy-dependent lifespan extension in *C. elegans*. PLoS One 8 (7), e70087.

Nomura, K.H., et al., 2011. Ceramide glucosyltransferase of the nematode Caenorhabditis elegans is involved in oocyte formation and in early embryonic cell division.

Glycobiology 21 (6), 834–848.
Owopetu, O., et al., 2016. Fatty acids composition of Caenorhabditis elegans using accurate mass GCMS-QTOF AU - Henry, Parise. J. Environ. Sci. Health B 51 (8), 546–552.
Perez, C.L., Van Gilst, M.R., 2008. A 13C isotope labeling strategy reveals the influence of insulin signaling on lipogenesis in C. Elegans. Cell Metab. 8 (3), 266–274.
Rao, W., Isaac, R.E., Keen, J.N., 2011. An analysis of the Caenorhabditis elegans lipid raft proteome using geLC-MS/MS. J. Proteomics 74 (2), 242–253.
Sedensky, M.M., et al., 2004. A stomatin and a degenerin interact in lipid rafts of the nervous system of Caenorhabditis elegans. Am. J. Physiol. Cell Physiol. 287 (2), C468–C474.
Shaner, R.L., et al., 2009. Quantitative analysis of sphingolipids for lipidomics using triple quadrupole and quadrupole linear ion trap mass spectrometers. J. Lipid Res. 50 (8), 1692–1707.
Simons, K., Ikonen, E., 1997. Functional rafts in cell membranes. Nature 387, 569.
Sud, M., et al., 2007. LMSD: LIPID MAPS structure database. Nucleic Acids Res. 35 (suppl 1), D527–D532.
Tsugawa, H., et al., 2017. Comprehensive identification of sphingolipid species by in silico retention time and tandem mass spectral library. J. Cheminform. 9 (1), 19.
von Reuss, S.H., Dolke, F., Dong, C., 2017. Ascaroside profiling of Caenorhabditis elegans using gas chromatography–Electron ionization mass spectrometry. Anal. Chem. 89 (19), 10570–10577.
Vrablik, T.L., et al., 2015. Lipidomic and proteomic analysis of Caenorhabditis elegans lipid droplets and identification of ACS-4 as a lipid droplet-associated protein. Biochim. Biophys. Acta (BBA) – Mol. Cell Biol. Lipids 1851 (10), 1337–1345.
Watts, J.L., Browse, J., 2002. Genetic dissection of polyunsaturated fatty acid synthesis in Caenorhabditis elegans. Proc. Natl. Acad. Sci. U. S. A. 99 (9), 5854–5859.
Watts, J.L., Ristow, M., 2017. Lipid and Carbohydrate Metabolism in *Caenorhabditis elegans*. Genetics 207 (2), 413–446.
Witting, M., et al., 2014. Optimizing a ultrahigh pressure liquid chromatography-time of flight-mass spectrometry approach using a novel sub-2 μm core–shell particle for in depth lipidomic profiling of Caenorhabditis elegans. J. Chromatogr. A 1359 (0), 91–99.
Zhu, H., et al., 2013. In: In: Ahringer, J. (Ed.), A Novel Sphingolipid-TORC1 Pathway Critically Promotes Postembryonic Development in Caenorhabditis elegans, vol. 2.